Model Predictive Controlled Active NPC Inverter for Voltage Stress Balancing Among the Semiconductor Power Switches

Md. Parvez Akter
School of Electrical and Information Engineering
The university of Sydney, NSW 2006, Australia
e-mail: md.akter@sydney.edu.au

Dylan Dah-Chuan Lu
School of Electrical, Mechanical & Mechatronic Systems
University of Technology Sydney, NSW 2007, Australia
e-mail: dylan.lu@uts.edu.au

***Abstract*—This paper presents a model predictive controlled three-level three-phase active neutral-point-clamped (ANPC) inverter for distributing the voltage stress among the semiconductor power switches as well as balancing the neutral-point voltage. The model predictive control (MPC) concept uses the discrete variables and effectively operates the ANPC inverter by avoiding any linear controller or modulation techniques. A 4.0 kW three-level three-phase ANPC inverter is developed in the MATLAB/Simulink environment to verify the effectiveness of the proposed MPC scheme. The results confirm that the proposed model predictive controlled ANPC inverter equally distributes the voltage across all the semiconductor power switches and provides lowest THD (0.99%) compared with the traditional NPC inverter. Moreover, the neutral-point voltage balancing is accurately maintained by the proposed MPC algorithm. Furthermore, this MPC concept shows the robustness capability against the parameter uncertainties of the system which is also analyzed by MATLAB/Simulink.**

Keywords- Model predictive control (MPC); active NPC inverter (ANPC); voltage stress balancing; neutral-point voltage balancing; stability and robustness.

I. INTRODUCTION

The neutral-point-clamped (NPC) inverter introduced in 1981 by Nabae [1], is the most widely used topology in widespread applications in various fields such as renewable energy generation [2], medium voltage drives [3] and electric vehicle traction [4]. This NPC inverter provides significant advantages over the two-level voltage source inverter (VSC), such as lower THD, higher power capability and smaller *dv*/*dt* and output inverter common mode voltages [5]. Aside from these several advantages, the NPC inverter faces some major limitations including the uneven voltage stress across the semiconductor power switches, neutral point voltage balancing and robustness against the parameter uncertainties. The uneven voltage stress across the power switches limits the switching frequency, maximize the entire phase current and reduce the output power of the NPC inverter [6]. This voltage stress problem is solved by using the active neutral-point-clamped (ANPC) which offers additional zero switching states by employing two active switches in every phase of the NPC inverter [7]. Moreover, the neutral point voltage balancing and the robustness problems are solved by using the model predictive control (MPC).

The MPC is a multidimensional constrained based control technique which solves the constrained finite time optimal control problems of the nonlinear systems at every sample time instant. MPC has gained significant attention in power converters and electrical drives research due to its intuitive approach, elimination of linear controllers and modulators, and easy inclusion of nonlinearities and restrictions [8-10]. Due to these various advantages, MPC has been implemented in different power converter topologies such as voltage source inverter [11], active-front-end rectifier [12-14], rectifier and inverter (ac-dc-ac) system [15], bidirectional ac-dc inverter [16, 17], direct matrix converter [18] and indirect matrix converter [19], etc. Although, some research has been done on using of MPC in NPC inverter [20, 21], complete investigation on the model predictive controlled three-level ANPC inverter, namely, ensuring the voltage stress distribution across the power switches, neutral-point voltage balancing and robust operation, is still yet to be done in the existing state-of-art.

A model predictive controlled three-level three-phase active neutral-point-clamped (ANPC) inverter for distributing the voltage stress among the semiconductor power switches as well as balancing the neutral-point voltage and improving the system performance is presented in this paper. The rest of the paper is structured as follows. The dynamic modeling of the ANPC inverter with MPC scheme is introduced in section II. Section II presents the simulation results and discussion in order to validate the proposed model predictive control scheme for three-level three-phase ANPC inverter. Moreover, the comparative evaluation between the proposed ANPC and the traditional NPC inverter and the robustness of the proposed MPC concept are analyzed in section IV. Finally, fruitful conclusions are drawn in section VIII.

II. MODELLING OF THE ANPC INVERTER WITH MPC

Fig. 1 shows the schematic system configuration which includes a three-level three-phase active neutral-point-clamped (ANPC) inverter and an inductive-resistive-active load. The ANPC inverter consists of 18 anti-parallel diode-clamped IGBT switches. Each phase-leg consists of six switches (S_{x1}-S_{x6}), where x is phase (a, b, or c). In this converter, the active switches S_{x5} and S_{x6}, and their associated anti-parallel diodes are clamped to neutral-point (o) which generates six switching states as shown in Table I, these are capable of generating three different voltage levels, namely, $+V_{dc/2}$, 0 (0U2, 0U1, 0L1, 0L2) and $-V_{dc/2}$. The space vector block diagram of the three-level ANPC inverter is presented in Fig. 2, in which all the zero states are replaced by Z. Therefore, for a three-level ANPC inverter, one can still utilize 27 switching states to express all the possible switching states, such as [1 Z Z].

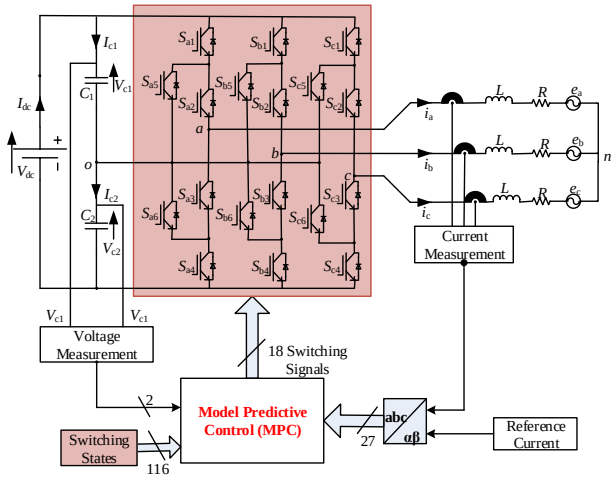

Figure 1. The ANPC inverter and its proposed MPC scheme.

A. *Mathemetical Modelling of the ANPC Inverter*

The power circuit of the ANPC inverter transfers the electrical power from dc voltage supply to three-phase inductive-resistive-active load as shown in the Fig. 1. The relation between the output voltage space vector ($\vec{v}_{\text{ANPC}}$), switching state function vector ($\vec{S}$) and the dc-link voltage (V_{dc}) of the NPC inverter can be presented as:

$$\vec{v}_{\text{ANPC}} = \vec{S} \times V_{\text{dc}} \tag{1}$$

Otherwise, the voltage vector ($\vec{v}_{\text{ANPC}}$) generated by the ANPC inverter is described with the phase to neutral voltages ($v_{\text{ao}}, v_{\text{bo}}$, and v_{co}) as:

$$\vec{v}_{\text{ANPC}} = \frac{2}{3}(v_{\text{ao}} + \vec{\omega} v_{\text{bo}} + \vec{\omega}^2 v_{\text{co}}) \tag{2}$$

where, $\vec{\omega} = e^{j2\pi/3}$, denotes 120° phase shift between the phases.

The three-level ANPC inverter is connected to the three-phase inductive-resistive-active ac load as shown in Fig. 1. Hence, the output space voltage vector dynamics generated by the inverter can be obtained as:

$$\begin{aligned}\vec{v}_{\text{ANPC}} = L\frac{d\vec{i}}{dt} + R\vec{i} + \frac{2}{3}\left(e_{\text{a}} + \vec{\omega} e_{\text{b}} + \vec{\omega}^2 e_{\text{c}}\right) \\ + \frac{2}{3}\left(v_{\text{no}} + \vec{\omega} v_{\text{no}} + \vec{\omega}^2 v_{\text{no}}\right)\end{aligned} \tag{3}$$

The ac load current ($\vec{i}$) and back-emf ($\vec{e}$) space vector model can be expressed as:

$$\vec{i} = \frac{2}{3}(i_{\text{a}} + \vec{\omega} i_{\text{b}} + \vec{\omega}^2 i_{\text{c}}) \tag{4}$$

and

$$\vec{e} = \frac{2}{3}(e_{\text{a}} + \vec{\omega} e_{\text{b}} + \vec{\omega}^2 e_{\text{c}}) \tag{5}$$

TABLE I. EACH PHASE SWITCHING STATES OF THE ANPC INVERTER

State	Switching Sequence						Voltage vector ($\vec{v}_{\text{ANPC}}$)	No	
	S_{x1}	S_{x2}	S_{x3}	S_{x4}	S_{x5}	S_{x6}			
+	1	1	0	0	0	1	$+V_{dc}/2$	**1**	
0U2	0	1	0	0	1	0	0	**2**	**Z**
0U1	0	1	0	1	1	0	0	**3**	
0L1	1	0	1	0	0	1	0	**4**	
0L2	0	0	1	0	0	1	0	**5**	
-	0	0	1	1	1	0	$-V_{dc}/2$	**6**	

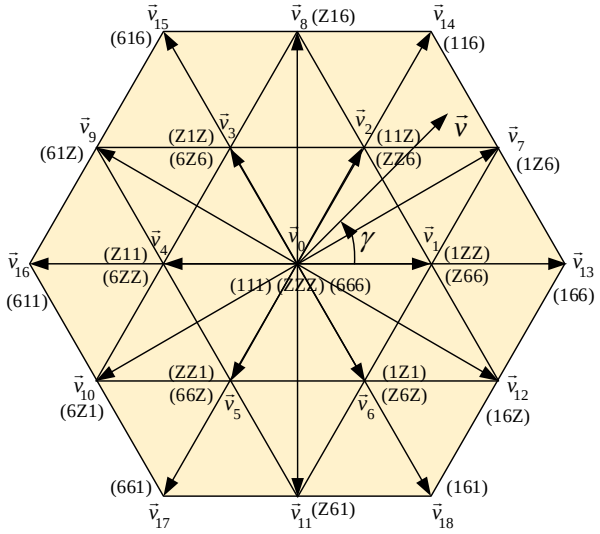

Figure 2. The space vector diagram of ANPC inverter.

where i_{a}, i_{b}, and i_{c} are the ac load phase currents and e_{a}, e_{b} and e_{c} are the back-emf phase voltages.

Then the load current dynamics of the three-level three-phase ANPC inverter can be presented from (3), (4) and (5) as the last term of (3) is zero. Hence the three-phase load current dynamics is:

$$L\frac{d\vec{i}}{dt} = \left(\vec{v}_{\text{ANPC}} - \vec{e}\right) - R\vec{i} \tag{6}$$

Finally, dynamics of the dc-link capacitor voltages (V_{c1} and V_{c2}) can be described with the capacitor current (i_{c1} and i_{c2}) as:

$$\frac{dV_{\text{c1}}}{dt} = \frac{1}{C} i_{\text{c1}} \text{ and } \frac{dV_{\text{c2}}}{dt} = \frac{1}{C} i_{\text{c2}} \tag{7}$$

where, C is the capacitor value.

B. *Dynamic discrete time model of the ANPC inverter*

The continuous time based dynamic system of the three-level three-phase ANPC inverter, as represented in (6) and (7), needs to transform into discrete time domain as the MPC is formulated in discrete time domain. Then, an appropriate cost function is derived from these discrete variables to achieve the controllability of the MPC technique for the ANPC inverter.

The dynamic discrete time model of the ANPC inverter is approximated with Euler equation $(dx/dt \approx \{x(k)-x(k-1)\}/T_s)$ at a sampling time T_s. By utilizing one step ahead of this Euler approximation, the discrete future predictive current ($\vec{i}(k+1)$) vector of the three-phase ANPC inverter can be derived from the continuous time current dynamic of (6) as:

$$\vec{i}(k+1)=\frac{1}{L+RT_s}\left\{L\vec{i}(k)+T_s\left[\vec{v}_{ANPC}(k+1)-\vec{e}(k+1)\right]\right\} \quad (8)$$

On the other hand, the discrete time model of the future dc-link capacitor voltages (k+1) are:

$$V_{c1}(k+1)=V_{c1}(k)+\frac{1}{C}i_{c1}(k)T_s \quad (9)$$

and

$$V_{c2}(k+1)=V_{c2}(k)+\frac{1}{C}i_{c2}(k)T_s \quad (10)$$

There are 27 future value of the three-phase load current ($\vec{i}(k+1)$), and the dc-link capacitor voltages (V_{c1} and V_{c2}) are predicted by the switching states of the ANPC inverter. Therefore, an appropriate cost function is essential for the MPC algorithm for the proper selection of the switching states. The cost function ($\vec{c}$) is evaluated for every switching states. The switching state that gives minimum value of the cost function is applied to the three-level three-phase ANPC inverter for operation and also uses during the next sampling instant. The cost function ($\vec{c}$) of the MPC scheme is defined with future measured reference load current ($\vec{i}_{ref}(k+1)$), predicted load current ($\vec{i}(k+1)$) and dc-link capacitor voltages ($V_{c1}(k+1)-V_{c2}(k+1)$) as:

$$\vec{c}=\left|\vec{i}_{ref}(k+1)-\vec{i}(k+1)\right|+\lambda_{dc}\left|V_{c1}(k+1)-V_{c2}(k+1)\right| \quad (11)$$

where, λ_{dc} is the weighting factor which maintains the voltage balance of the two dc-link capacitor voltages.

C. Control *scheme*

Fig. 1 shows the MPC strategy for three-level ANPC inverter. The load current ($\vec{i}(k)$) is measured and the future predicted current $(\vec{i}(k+1))$ is calculated by utilizing (9) for each one of 116 possible switching state function vector ($\vec{S}$) of the converter. This future value ($\vec{i}(k+1)$) is compared with reference load current ($\vec{i}_{ref}(k+1)$) of the NPC inverter by using cost function ($\vec{c}$) of equation (11). Finally, the switching states ($\vec{S}$) of the three-level three-phase ANPC inverter which minimizes the cost function ($\vec{c}$), is selected for next sampling time. Moreover, the voltage balancing between the two capacitor voltages $(V_{c1}(k+1)-V_{c2}(k+1))$ is also achieved by utilizing the cost function in (11).

TABLE II. SIMULATION PARAMETERS

Variables and Parameters	Values	Units
Power Rating (P)	4.0	kW
DC-link Voltage (V_{dc})	533	V
Load inductance (L_s)	30	mH
Load resistance (Rs)	10	Ω
Capacitor (C_1, C_2)	750	μF
Sampling time (T_s)	50	μs

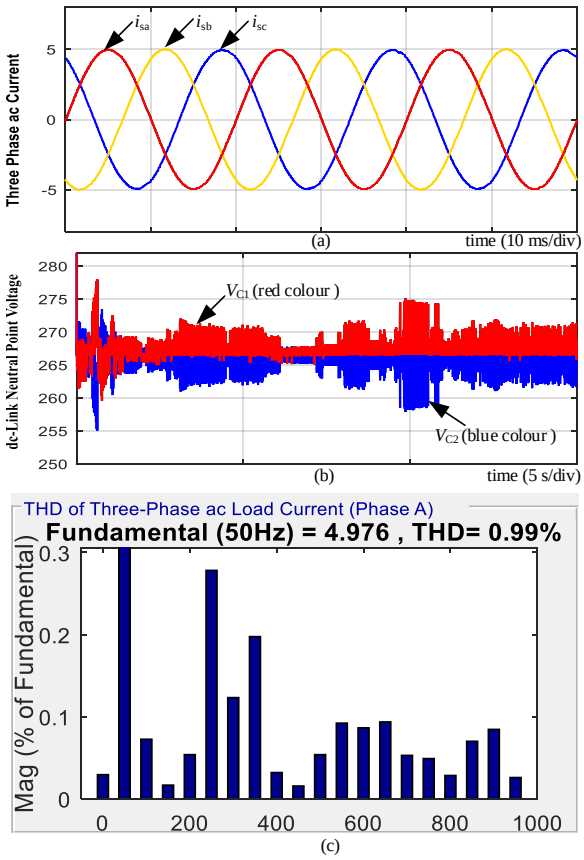

Figure 3. Simulation results of model predictive controlled ANPC inverter: (a) three-phase ac load current, (b) neutral point voltage and (c) THD of the load current (phase A).

III. SIMULATION RESULTS

The proposed model predictive controlled ANPC scheme is simulated in MATLAB/Simulink to validate efficacy of the system. Parameters used in simulation are listed in Table II and the simulation result is presented in Fig.3. The three-phase load current drawn by the MPC controlled ANPC inverter is depicted in Fig. 3(a). The reference load current is set at a value of 5 A (peak) for each phase and the Fig. 3(a) demonstrates that, each phase load current $\vec{i}(k+1)$ is accurately tracking the reference value $(\vec{i}_{ref}(k+1))$, which verifies the feasibility of the model predictive control method. Furthermore, the MPC algorithm effectively reduces

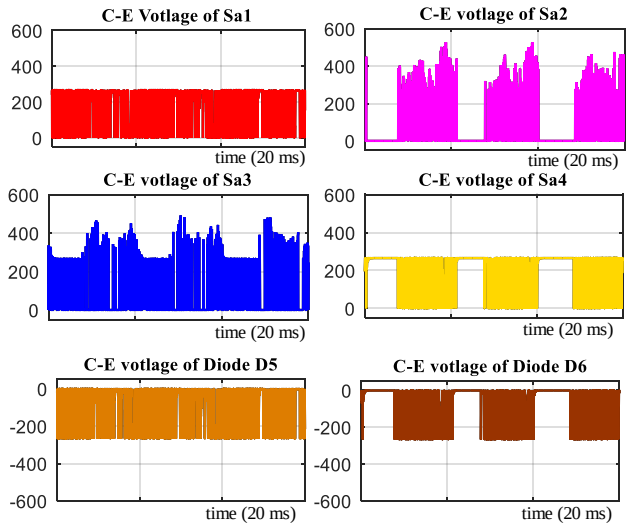

Figure 4. Simulation results of voltages across the semiconductor power switches and the diodes of the model predictive controlled NPC inverter (Phase A).

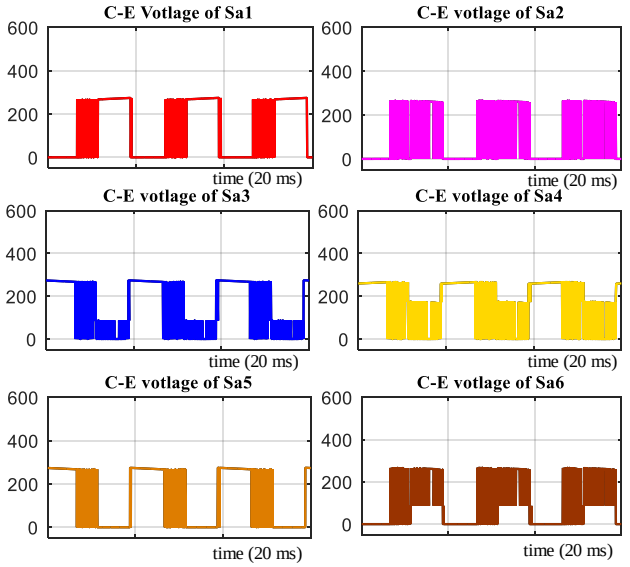

Figure 5. Simulation results of voltages across the semiconductor power switches of the model predictive controlled ANPC inverter (Phase A).

the THD of load current by accurately tracking the sinusoidal reference current. Fig. 3(c) confirms that the total harmonic distortion (THD) of the model predictive controlled ANPC inverter is 0.99%, which can be accepted as a very good performance.

Additionally, another important outcome of the proposed MPC algorithm is to balance the neutral-point voltage of the ANPC inverter. This neutral-point voltage can be denoted as the difference between the two dc-link capacitor voltages. The Fig. 3(b) shows two dc-link capacitor voltages (V_{c1} and V_{c2}), which confirms that the neutral-point voltage of the ANPC inverter is accurately balanced. The value of the weighting factor is fixed at $\lambda_{dc} = 0.01$, to achieve the best performance.

IV. Comparative Evaluation and Robustness Analysis

A. *Comparative Evaluation*

A comparative evaluation is performed in this section to verify the efficacy of the proposed MPC controlled ANPC inverter over its traditional NPC inverter. One of the major aim of this research is to balance and equalize the voltage stress among all the semiconductor power switches of the inverter. Fig. 4 shows the voltages across the semiconductor power switches ($S_{a1} - S_{a4}$) and the diodes ($D_5 - D_6$) of phase A of the model predictive controlled NPC inverter. The simulation result shows that there is uneven voltage stress among the power switches of the NPC inverter which further cause the unequal power loss and failure of the devices. In order to overcome this problem, MPC controlled ANPC inverter is proposed. Fig. 5 presents the collector-emitter voltages of the IGBT power switches ($S_{a1} - S_{a6}$) of phase A, which confirms that all the power switches of the ANPC inverter face equal voltage stress.

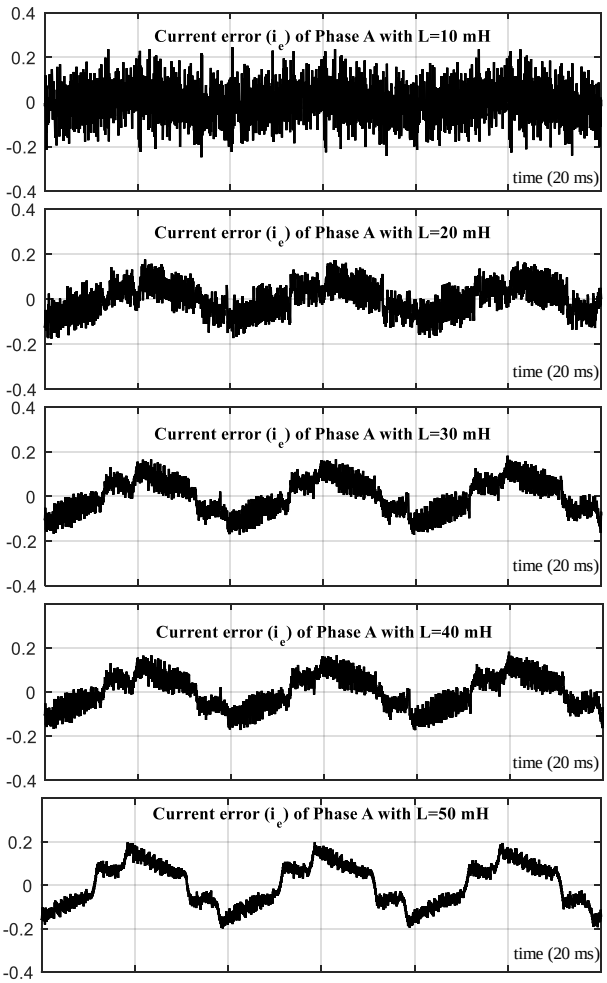

Figure 6. Robustness analysis of the proposed MPC scheme with the variation of current error in case of parameter uncertainties.

B. Robustness Analysis

The robustness of the proposed MPC algorithm is analyzed against the filter parameters uncertainties of the three-level ANPC inverter. Fig. 6 shows the current error variation ($\vec{i}_{\mathrm{e}} = \vec{i} - \vec{i}_{\mathrm{ref}}$) with the variation of filter parameters. The maximum deviation of the current error ($\vec{i}_{\mathrm{e}}$) is limited within 0.2 A (less than 4% which is negligible) which confirms the robustness of the proposed scheme. This current deviation against the filter parameter variation is verified in MATLAB/Simulink software. The equation for the calculation of current deviation used in this section is as follows:

$$\vec{i}_{\mathrm{e}} = \{(\vec{i} - \vec{i}_{\mathrm{ref}}) / \vec{i}_{\mathrm{ref}}\} \times 100\% \quad (12)$$

V. Conclusions

A model predictive controlled three-level three-phase active neutral-point-clamped (ANPC) inverter is presented in this paper to equally distribute the voltage stress among all the semiconductor power switches. The proposed concept is enhanced by deriving a cost function which provides very good system performance as well as ensures the robustness. Moreover, the dc-link capacitor voltage balance is also accurately maintained by the proposed controller at all time. The simulation results of three-phase ANPC inverter strongly agree and show very good system performance. Again, the MPC also shows the robustness capability with the parameter uncertainties, which is verified by the robustness analysis in against filter parameter variation. The results associated in this investigation are very encouraging and will continue to play a strategic role in the equal loss distribution among all the power switches and fault-tolerant capability of the modern high-performance active neutral-point-clamped (ANPC) inverters.

Acknowledgment

The authors would like to thank the Australian Government and the University of Sydney for providing financial support through the 2016 International Postgraduate Research Scholarships (IPRS).

References

[1] A. Nabae, I. Takahashi, and H. Akagi, "A new neutral-point-clamped PWM inverter," *IEEE Trans. Ind. Appl.*, pp. 518-523, 1981.

[2] S. Kouro, J. I. Leon, D. Vinnikov, and L. G. Franquelo, "Grid-connected photovoltaic systems: An overview of recent research and emerging PV converter technology," *IEEE Ind. Electron. Magazine*, vol. 9, pp. 47-61, 2015.

[3] J. Rodríguez, S. Bernet, B. Wu, J. O. Pontt, and S. Kouro, "Multilevel voltage-source-converter topologies for industrial medium-voltage drives," *IEEE Trans. Ind. Electron.*, vol. 54, pp. 2930-2945, 2007.

[4] A. Choudhury, P. Pillay, and S. S. Williamson, "Modified DC-Bus Voltage-Balancing Algorithm Based Three-Level Neutral-Point-Clamped IPMSM Drive for Electric Vehicle Applications," *IEEE Trans. Ind. Electron.*, vol. 63, pp. 761-772, 2016.

[5] X. Jing, J. He, and N. A. Demerdash, "Loss balancing SVPWM for active NPC converters," in *Proc. IEEE Applied Power Electron. Conf. and Expo. (APEC-2014)*, 2014, pp. 281-288.

[6] T. Bruckner, S. Bernet, and H. Guldner, "The active NPC converter and its loss-balancing control," *IEEE Trans. Ind. Electron.*, vol. 52, pp. 855-868, 2005.

[7] S. R. Pulikanti, M. S. Dahidah, and V. G. Agelidis, "Voltage balancing control of three-level active NPC converter using SHE-PWM," *IEEE Trans. Power Delivery*, vol. 26, pp. 258-267, 2011.

[8] M. P. Akter, S. Mekhilef, N. M. L. Tan, and H. Akagi, "Modified Model Predictive Control of a Bidirectional ac-dc Converter Based on Lyapunov Function for Energy Storage Systems," *IEEE Trans. Ind. Electron.*, vol. 63, pp. 704-715, 2016.

[9] M. Rivera, J. Rodriguez, and S. Vazquez, "Predictive control in power converters and electrical drives- part ii," *IEEE Trans. Ind. Electron.*, vol. 63, pp. 4472-4474, 2016.

[10] J. Rodriguez, M. P. Kazmierkowski, J. R. Espinoza, P. Zanchetta, H. Abu-Rub, H. A. Young, *et al.*, "State of the Art of Finite Control Set Model Predictive Control in Power Electronics," *IEEE Trans. Ind. Info.*, vol. 9, pp. 1003-1016, 2013.

[11] S. Kwak and S. k. Mun, "Model Predictive Control Methods to Reduce Common-Mode Voltage for Three-Phase Voltage Source Inverters," *IEEE Trans. Power Electron.*, vol. 30, pp. 5019-5035, 2015.

[12] M. P. Akter, S. Mekhilef, N. M. L. Tan, and H. Akagi, "Stability and performance investigations of model predictive controlled active-front-end (AFE) rectifiers for energy storage systems," *Journal of Power Electron.*, vol. 15, pp. 202-215, 2015.

[13] M. Parvez, S. Mekhilef, N. M. Tan, and H. Akagi, "An improved active-front-end rectifier using model predictive control," in *Proc. IEEE Applied Power Electron. Conf. and Expo. (APEC-2015)*, 2015, pp. 122-127.

[14] M. Parvez, S. Mekhilef, N. M. Tan, and H. Akagi, "A robust modified model predictive control (MMPC) based on Lyapunov function for three-phase active-front-end (AFE) rectifier," in *Proc. IEEE Applied Power Electron. Conf. and Expo. (APEC-2016)*, 2016, pp. 1163-1168.

[15] D. Zhou, J. Zhao, and Y. Li, "Model-Predictive Control Scheme of Five-Leg AC-DC-AC Converter-Fed Induction Motor Drive," *IEEE Trans. Ind. Electron.*, vol. 63, pp. 4517-4526, 2016.

[16] M. P. Akter, S. Mekhilef, N. M. L. Tan, and H. Akagi, "Model predictive control of bidirectional AC-DC converter for energy storage system," *J. Electr. Eng. and Tech.*, vol. 10, pp. 165-175, 2015.

[17] M. Parvez, S. Mekhilef, N. M. Tan, and H. Akagi, "Model predictive control of a bidirectional AC-DC converter for V2G and G2V applications in electric vehicle battery charger," in *Proc. IEEE Transportation Electrification Conf. and Expo. (ITEC-2014)*, 2014, pp. 1-6.

[18] M. Rivera, C. Rojas, J. Rodr, x00Ed, guez, P. Wheeler, *et al.*, "Predictive Current Control With Input Filter Resonance Mitigation for a Direct Matrix Converter," *IEEE Trans. Power Electron.*, vol. 26, pp. 2794-2803, 2011.

[19] J. L. Elizondo, A. Olloqui, M. Rivera, M. E. Macias, O. Probst, O. M. Micheloud, *et al.*, "Model-Based Predictive Rotor Current Control for Grid Synchronization of a DFIG Driven by an Indirect Matrix Converter," *IEEE Journal of Emerging and Selected Topics in Power Electron.*, vol. 2, pp. 715-726, 2014.

[20] A. Calle-Prado, S. Alepuz, J. Bordonau, J. Nicolas-Apruzzese, P. Cortés, and J. Rodriguez, "Model predictive current control of grid-connected neutral-point-clamped converters to meet low-voltage ride-through requirements," *IEEE Trans. Ind. Electron.*, vol. 62, pp. 1503-1514, 2015.

[21] M. Narimani, B. Wu, V. Yaramasu, and N. R. Zargari, "Finite Control-Set Model Predictive Control (FCS-MPC) of Nested Neutral Point-Clamped (NNPC) Converter," *IEEE Trans. Power Electron.*, vol. 30, pp. 7262-7269, 2015.